Epitaxial crystallization and crystalline polymorphism of poly(1-butene): forms III and II

S. Kopp, J. C. Wittmann and B. Lotz*
Institut Charles Sadron, CNRS-ULP, 6 rue Boussingault, 67083 Strasbourg Cedex, France
(Received 20 April 1993; revised 13 July 1993)

The three crystalline phases of isotactic poly(1-butene), which differ by their helix conformation and unit cell parameters, are obtained by bulk crystallization via epitaxy on appropriate organic substrates, in particular aromatic acids or salts. In this paper, the epitaxial relationships between forms III and II are established, based on composite electron diffraction patterns where possible. Form III epitaxy rests mainly on the matching of the chain axis repeat distance; form II is an original illustration of an epitaxy of irrational helices in which the interturn distance plays the main role.

(Keywords: poly(1-butene); crystal polymorphism; epitaxy)

INTRODUCTION

The epitaxial crystallization of polymers on alkali halides or on low-molecular-weight organic compounds and salts can result in oriented growth of unstable crystalline phases, or phases that are not formed spontaneously: examples include polyethylene (PE), which can be obtained in its unstable monoclinic modification[1,2], and isotactic polypropylene (iPP), which can be obtained in its less common β modification (when nucleated with the organic pigment γ-chinacridone[3]). In both cases, however, these phases have the *same chain conformation* (i.e. planar zigzag and ternary helix, for PE and iPP, respectively) as the stable phases, and differ only in their packing, i.e. by the *different interchain distances.* These altered distances provide a better fit with the substrate lattice periodicities and cause the observed epitaxially induced polymorphism.

Isotactic poly(1-butene) (PBu1) crystallizes in different phases with *different chain conformations* and, as a consequence, different unit cell geometries and symmetries[4]. Form I′ (3_1 helix) has a hexagonal (trigonal) unit cell (space group R3c or R$\bar{3}$c), with the parameters, $a = b = 1.77$ nm, $c = 0.65$ nm and $\gamma = 120°$. A closely related form I (same helix geometry and unit cell dimensions) is obtained by a spontaneous solid-state transformation of form II. Form II (11_3 helix) has a tetragonal unit cell with the parameters $a = b = 1.542$, and $c = 2.105$ nm, and has P$\bar{4}$ symmetry. (The unit cell determined by Petraccone *et al.*[5] is used in the following rather than the slightly different one proposed by Turner-Jones[6].) Form III (4_1 helix) has an orthorhombic unit cell with the parameters $a = 1.238$, $b = 0.888$, and $c = 0.756$ nm, and the space group $P2_12_12_1$. Bulk crystallization at atmospheric pressure yields form II, which transforms spontaneously to form I over periods of days or weeks. Forms III and I′ are obtained by crystallization from solution. The latter, denser form is also obtained by bulk crystallization under high pressure.

In the context of epitaxial crystallization. PBu1 therefore provides a new challenge, in that direct formation of the less common phases involves not only different packings, (i.e. the intermolecular energy balance), but also different *conformations of chains* in interaction with the substrate (i.e. the intramolecular energy balance).

In this present set of papers, we report on the successful epitaxial crystallization of the three crystalline phases of PBu1 from the bulk and at atmospheric pressure. The substrates used are low-molecular-weight organic compounds, which provide a broad palette of repeat distances and surface structures[7]. The epitaxial relationships are established by the analysis of selected-area electron diffraction patterns, sometimes on composite polymer–substrate bilayers. This analysis is developed here for forms III and II. For form I′, which is considered in a companion paper[8], the analysis can be carried over to the determination of the hand of the helices interacting with the substrate.

EXPERIMENTAL

Samples

A high-molecular-weight (M_w) poly(1-butene) sample purchased from Aldrich ($M_w \sim 180\,000$) has generally been used in this work. A low-M_w sample, obtained by fractionation of a laboratory material, was also used. Since epitaxial crystallization is governed by interactions at the unit cell level, no significant differences in behaviour are observed for the two samples. The fraction is preferred whenever low-melting substrates are used, given its lower melting temperature (~100°C *versus* 115°C for form I).

All substrates are of commercial origin. Salts are obtained from the acids by reaction with the corresponding dilute bases and are recrystallized by evaporation from ethanolic solutions.

---

* To whom correspondence should be addressed

0032-3861/94/05/0908-08

Sample preparation and examination

The preparation of samples suitable for electron microscopy and electron diffraction studies is based on various techniques developed in our laboratory, details of which have been reported elsewhere[9].

When the substrates have high melting temperatures and can solubilize the polymer, mixing is achieved by co-melting between two glass slides, with crystallization being induced by sliding (to a lower temperature) on a Kofler bench. Separation of the cover slides and dissolution of the substrate with an organic solvent (e.g. ethanol) leaves a thin polymer film on each glass slide with the contact face with the former substrate exposed. When required, this film is gold decorated under normal incidence, carbon-coated, floated off on water with the help of a poly(acrylic acid) backing, and then mounted on copper grids.

When the substrates are infusible or when their melting temperatures are too high (e.g. for aromatic acid salts), a thin film of PBu1 is cast onto the glass slides by evaporation of a *p*-xylene solution. Crystals of the salts are then produced directly on the film by evaporation of an ethanolic solution. Alternatively, the crystals produced in suspension are simply deposited and the solvent is evaporated. Melting and recrystallization of the PBu1 film is then performed in the presence of the salt crystals; the latter are redissolved, again leaving a thin PBu1 film with imprints of the salt crystals and the PBu1 contact face exposed. The oriented film is then handled as above (optional gold decoration prior to the carbon backing process).

The films are examined either with a Hitachi HU11CS or a Philips CM12 microscope, the latter equipped with an eucentric goniometric rotation-tilt stage. The acceleration voltages used are 75 and 120 kV, respectively. Photographic plates are either Agfa Scientia or Agfapan APX100. Examination is performed under low illumination in view of the high sensitivity of PBu1 to electron beam damage.

Molecular modelling

Computer generated molecular modelling of the structure and the contact faces was carried out by using the Cerius molecular modelling software package for materials research (Molecular Simulations Inc. of Burlington, MA, and Cambridge, UK), run on a Silicon Graphics Station.

RESULTS AND DISCUSSION

The epitaxial crystallization of PBu1 has been achieved on a variety of materials, and the three crystalline forms have been obtained directly with the appropriate substrates. The majority of these substrates induce only one phase. In some cases, however, two phases are formed simultaneously; the relative proportion of these phases may be altered by using related, but different, substrates.

The epitaxies of all three phases, with the corresponding substrates that were used, are presented in *Table 1*. Note that all of the substrates have a common 'sandwich' structure consisting of non-polar and polar moieties. The crystals are arranged in sheets, with weak interactions between the adjacent apolar moieties leading to large contact planes lined up with the aromatic or substituted aromatic rings.

The rather straightforward epitaxy of form III is presented first, while the epitaxy of form II containing irrational helices, and its transformation to form I, is described next. The epitaxy of form I′, and an analysis of the chirality of the helices which interact with the substrate, is presented in a companion paper[8].

Epitaxial crystallization of PBu1, form III (PBu,III)

Form III of PBu1 has been obtained on one substrate only, namely 2-quinoxalinol (2Qxol), which has the molecular structure:

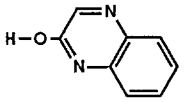

Table 1 Summary of the epitaxies of the three phases of PBu1 and the respective substrates used, both in this present work and in the companion study[8]

Substrate (abbreviation)	PBu1 crystalline phase	Number of orientation	Epitaxial relationships[a]
2-Quinoxalinol	III	1	$(110)_{\mathrm{PBu,III}} \parallel (001)_{\mathrm{2Qxol}}$
(2Qxol)			$c_{\mathrm{PBu,III}} \parallel [010]_{\mathrm{2Qxol}}$
Benzoic acid	II	2 (94°)	(100) or $(010)_{\mathrm{PBu,II}} \parallel (011)_{\mathrm{BzAc}}$
(BzAc)			$c_{\mathrm{PBu,II}} \parallel [110]_{\mathrm{PBu,II}}$ or $[\bar{1}10]_{\mathrm{BzAc}}$
4-Bromobenzoic acid	II	2 (50°)	Major: (100) or $(010)_{\mathrm{PBu,II}} \parallel (100)_{\mathrm{4BrBzAc}}$
(4BrBzAc)	(major)		$c_{\mathrm{PBu,II}} \parallel [032]$ or $[03\bar{2}]_{\mathrm{4BrBzAc}}$
	I′	2 (22°)	Minor: $(110)_{\mathrm{PBu,I'}} \parallel (100)_{\mathrm{4BrBzAc}}$
	(minor)		$c_{\mathrm{PBu,I'}} \Lambda [001]_{\mathrm{4BrBzAc}} = \pm 11^\circ$
4-Chlorobenzoic acid	I′	1 or	$(11.0)_{\mathrm{PBu,I'}} \parallel (100)_{\mathrm{4ClBzAc}}$
(4ClBzAc)	(major)	2 (22°)	$c_{\mathrm{PBu,I'}} \Lambda [001]_{\mathrm{4ClBzAc}} = \pm 11^\circ$
	II	1	$(100)_{\mathrm{PBu,II}} \parallel (100)_{\mathrm{4ClBzAc}}$
	(minor)		$c_{\mathrm{PBu,II}} \parallel [032]_{\mathrm{4ClBzAc}}$
Potassium hydrogen 4-chlorobenzoate	I′	2 (60°)	$(11.0)_{\mathrm{PBu,I'}} \parallel (100)_{\mathrm{KH4Cl\Phi}}$
(KH4ClΦ)			$c_{\mathrm{PBu,I'}} \Lambda [001]_{\mathrm{KH4Cl\Phi}} = \pm 30^\circ$
Potassium 4-chlorobenzoate	I′	2 (60°)	$(11.0)_{\mathrm{PBu,I'}} \parallel (100)_{\mathrm{4Cl\Phi COOK}}$
(4ClΦCOOK)			$c_{\mathrm{PBu,I'}} \Lambda [001]_{\mathrm{4Cl\Phi COOK}} = \pm 30^\circ$
Potassium 4-bromobenzoate	I′	2 (60°)	$(11.0)_{\mathrm{PBu,I'}} \parallel (100)_{\mathrm{4Br\Phi COOK}}$
(4BrΦCOOK)			$c_{\mathrm{PBu,I'}} \Lambda [001]_{\mathrm{4Br\Phi COOK}} = \pm 30^\circ$

[a] Λ represents angular relationship; for details see ref. 8

2Qxol melts (with decomposition) at 273°C. The unit cell is orthorhombic (space group $P2_12_12_1$), with cell parameters $a=0.4354$, $b=0.7348$ and $c=2.132$ nm (*Figure 1a*)[10]. The most logical cleavage plane, and thus the contact plane involved in the epitaxy, is the (001) or *ab* plane. Its surface structure is essentially a parallel array of benzene rings which stand almost edge-on (*Figure 1b*).

2Qxol was selected *a priori* as a possible substrate for form III, based on (i) an anticipated good match of its *b*-axis repeat distance (0.7348 nm) with the chain axis repeat distance of form III (0.756 nm)[11], and (ii) a possible second lattice match involving $2 \times a_{\mathrm{Qxol}} = 0.8708$ nm and the interhelical distance along the *b* parameter of form III (0.888 nm).

The epitaxial crystallization of PBu1 on small single crystals of 2Qxol, produced by crystallization from a dilute $CHCl_3$ solution giving crystals of $\sim 5\,\mu$m lateral dimensions, does indeed yield form III. *Figure 2a* shows a composite diffraction pattern of a substrate–polymer bilayer, in which the sharp spots and arced reflections are due to 2Qxol and PBu1, respectively. *Figure 2b* is a similar pattern after dissolution of the 2Qxol substrate.

These diffraction patterns confirm the formation of form III (e.g. the strong meridional 004 reflection on the fourth layer line) and the anticipated match of $c_{\mathrm{PBu,III}}$ and b_{2Qxol}. This match is particularly prominent in *Figure 2a* where substrate and polymer reflections are organized on the same layer lines.

However, the epitaxial relationship differs slightly from that anticipated in terms of the polymer contact plane that is involved. Indeed, on the equator of *Figure 2b*, by far the most prominent reflections are at 0.508 nm^{-1}, indexed as 210, and on the first layer line at spacings of 0.422 and 0.241 nm^{-1}, indexed as 211 and 421, respectively. The contact plane is thus $(110)_{\mathrm{PBu,III}}$ which is very nearly normal to (210) (the calculated angle is 91.2°). The epitaxial relationship can be summarized by:

$$(110)_{\mathrm{PBu,III}} \| (001)_{\mathrm{2Qxol}}$$

$$[001]_{\mathrm{PBu,III}} \| [010]_{\mathrm{2Qxol}}$$

A near-perfect dimensional match exists along the chain axis direction, i.e.

$$\frac{c_{\mathrm{PBu,III}} - b_{\mathrm{2Qxol}}}{b_{\mathrm{2Qxol}}} = \frac{0.756 - 0.7348}{0.7348} = 2.88\%$$

but is much poorer along the interchain direction. Indeed, one must suppose that the 0.762 nm interchain distance

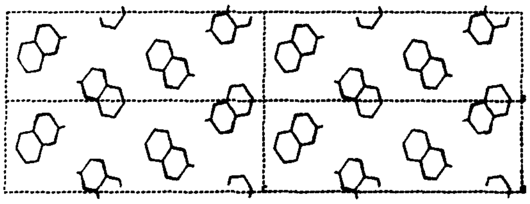

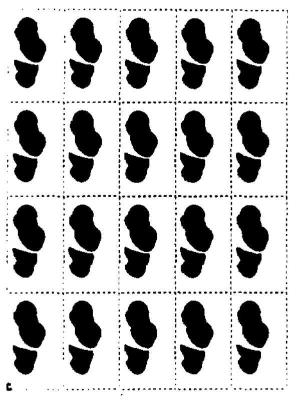

Figure 1 Computer generated molecular model of the 2-quinoxalinol crystal structure: (a) (100) plane projection and; (b) surface of the (001) plane which is in contact with the polymer

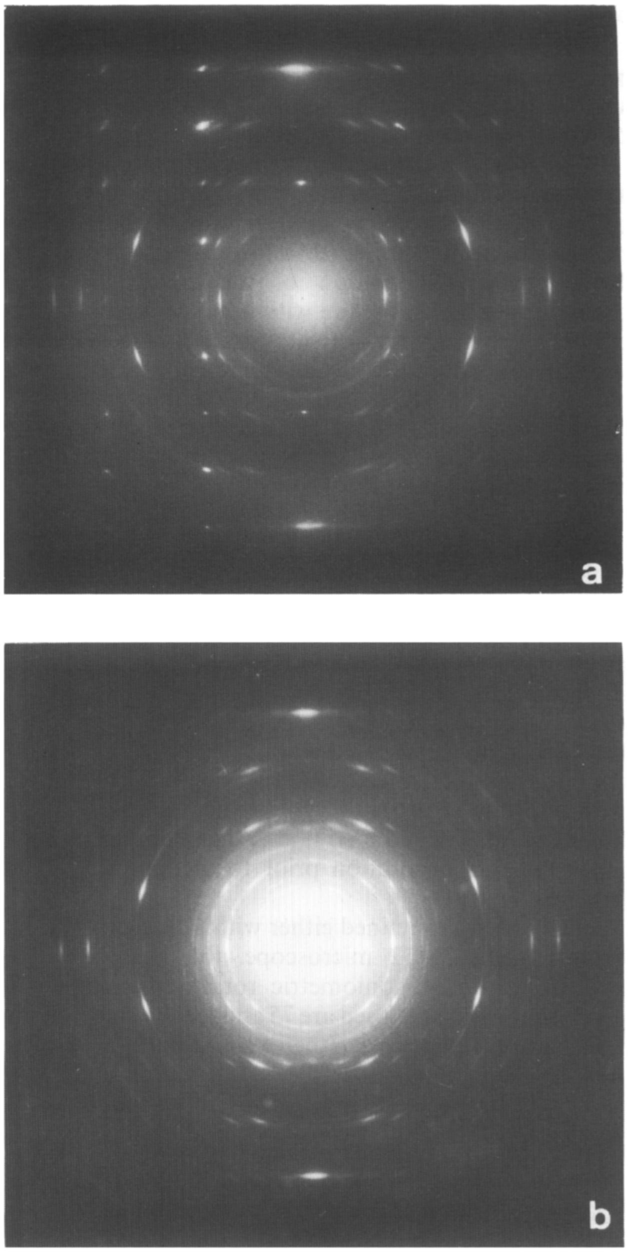

Figure 2 (a) Composite selected-area electron diffraction pattern of 2Qxol with PBu1, form III, epitaxially oriented on it, where the sharp and arced spots correspond to diffraction by the substrate and polymer, respectively. Polymer chain orientation and substrate b-axis are vertical. Note the position of the polymer and substrate diffraction spots on the same layer lines, indicating a good match. (b) Selected-area electron diffraction pattern of PBu1, form III, oriented on 2Qxol, after dissolution of the substrate. Note the strong meridional spot on the fourth layer line, indicating a 4_1 helix conformation

in the (110) plane of PBu,III 'interacts' with $2a_{2\mathrm{Qxol}}$, which sets the lattice match to ~12.5%, a value close to the accepted limits for an epitaxial relationship. It is certainly poorer than the match of $b_{\mathrm{PBu,III}}$ and $2a_{2\mathrm{Qxol}}$, had (100) been the contact plane (near-perfect match of +1.1%).

Selection of the actual (110) plane may tentatively be accounted for by noting that:

(i) The (110) plane is denser than the (100) plane (interchain distance of 0.762 nm, as opposed to 0.888 nm).

(ii) In this plane, side chains which are susceptible to interaction with the substrate are also much denser. As shown in *Figure 3a*, the ethyl side-chain arrangement is such that either the whole groups themselves, or their terminal CH_3 groups, are concentrated in planes parallel to the (110) plane. Assuming that the crystal structure is not significantly affected in the contact plane, a slice, 0.22 nm thick, which is parallel to (110), can be singled out: this represents the molecular subgroups most directly involved in the epitaxy. As seen in *Figure 3b*, these ethyls and terminal methyls are arranged in 'layers', nearly normal to the chain axis direction. Correspondence and complementarity with the substrate structure (cf. *Figure 1b*) are clearly apparent. By contrast, a similar representation of a (100) contact face indicates a much looser, less regular pattern of interacting side chains.

The lamellar morphology of epitaxially crystallized thin films is best revealed by gold decoration[12], since gold particles concentrate in interlamellar regions: *Figure 4* represents a small area of PBu,III which

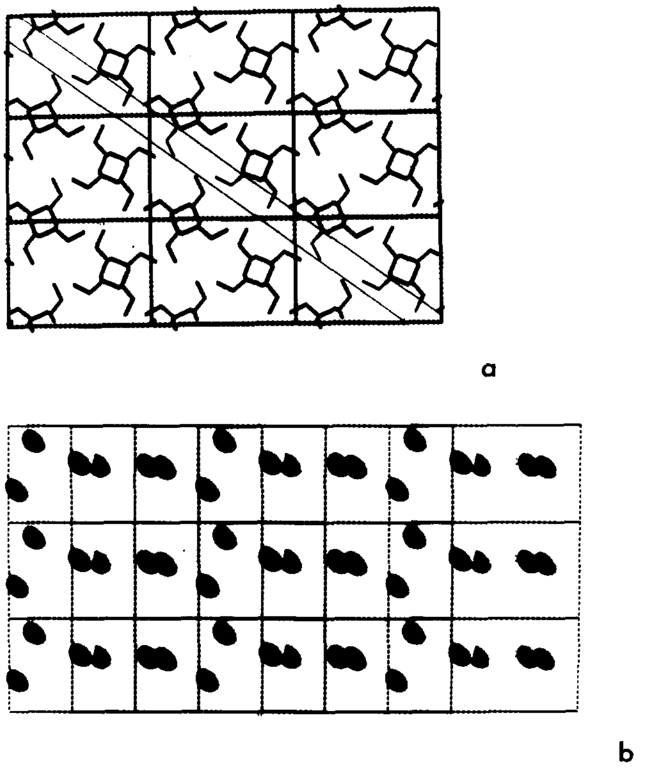

Figure 3 Molecular model of the unit cell of PBu1, form III: (a) (001) or *ab* plane, with indication of a slice through the structure parallel to the (110) contact plane and; (b) surface structure of the (110) contact plane of PBu1, with only atoms of the slice shown in (a) being represented

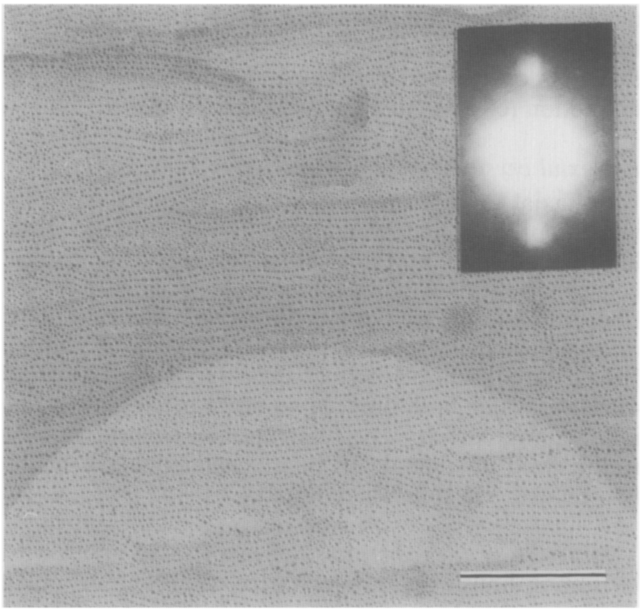

Figure 4 Electron micrograph of gold decorated PBu1, form III, epitaxially crystallized on 2Qxol: scale bar = 0.2 μm. Inset shows the low-angle diffraction pattern of the area selected (lighter zone)

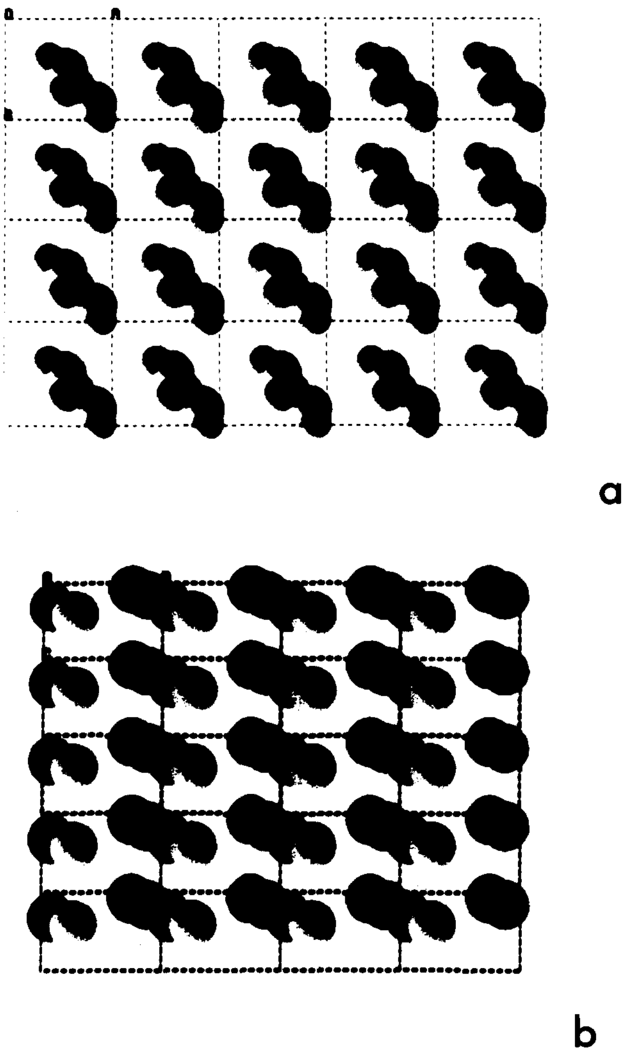

Figure 5 Computer generated molecular models of the contact surfaces (only the upper half of the benzene rings are shown) of: (a) the benzoic acid (001) plane and; (b) the 4-bromobenzoic acid (100) plane, where the bromine atoms appear as light areas

displays nearly parallel lamellae, as anticipated from the unique chain axis orientation. The average lamellar thickness, determined by selected-area, low-angle electron diffraction (cf. inset to *Figure 4*) is nearly 9 nm.

Epitaxial crystallization of PBul, form II (PBu,II)

Epitaxial crystallization of form II, namely the form which is produced spontaneously on bulk crystallization, has been achieved on three substrates, i.e. phenanthrene, benzoic acid (BzAc) and 4-bromobenzoic acid (4BrBzAc). Phenanthrene induces one chain orientation only, but, due to its low melting point, can be used only with low-M_w PBu1. We concentrate here on the epitaxies on BzAc and 4BrBzAc which both induce two chain orientations. The interactions, which involve irrational helices, can be rationalized in some detail by a parallel analysis of the two related, but different, epitaxies.

Structure of the substrates. Benzoic acid appears to be isomorphous with its monovalent salts (Na^+, K^+, etc.), which are familiar nucleating agents for crystallizable polymers. It is preferred in structural investigations as a result of a crystal morphology consisting of long, flat needles, which facilitates electron microscopy observations.

BzAc crystallizes in a monoclinic unit cell with the following parameters: $a=0.551$, $b=0.5157$, and $c=2.1973$ nm; $\beta=97.41°$; space group = $P2_1/c$[13]. The structure consists of layers of dimers of BzAc linked by pairs of hydrogen bonds. The (001) cleavage planes and contact planes are made up of the apolar benzene rings which stand edge-on on the surface (*Figure 5a*).

4BrBzAc has a similar structure and is made up of layers of dimers arranged in a monoclinic unit cell with the following parameters: $a=2.959$, $b=0.615$, and $c=0.398$ nm; $\beta=95.5°$; space group = $P2_1/a$[14]. The (100) cleavage and contact planes are populated with bromine atoms in position 4 and hydrogen atoms in position 3 of the benzene ring, the plane of which is nearly normal to the (100) and parallel to the (011) planes (see *Figure 5b*).

Epitaxies of PBul on BzAc and 4BrBzAc. PBu1 crystallizes epitaxially on both substrates, mainly as form II. Since both acids sublime under vacuum and are not amenable to electron microscopy examination, no composite substrate–polymer diffraction patterns are available. The epitaxial relationships must be established with the help of the substrate crystal morphologies and the complementary information provided by a second, minor PBu1 epitaxy in form I′.

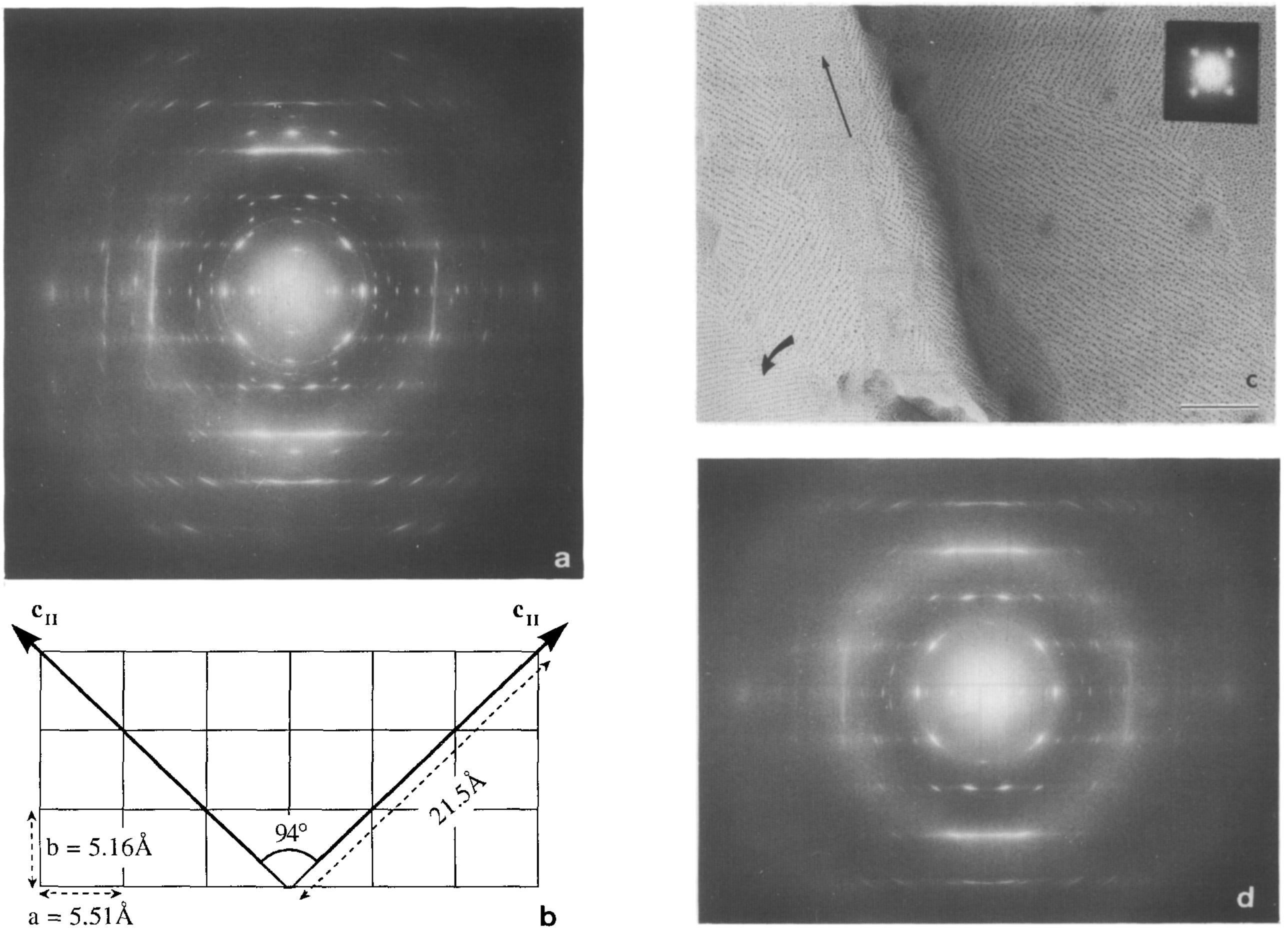

Figure 6 (a) Selected-area diffraction pattern of PBu1, epitaxially oriented on benzoic acid. Note the two orientations of the chains, 94° apart, and the presence of PBu1, form II (second internal diffraction spot on the equator corresponding to 200 at 0.745 nm^{-1}) and the early tranformation of this form into form I (internal diffraction spot corresponding to $1\bar{1}0$ at 0.888 nm^{-1}); (b) schematic representation of the PBu1, form II orientations, relative to the BzAc lattice (rotated clockwise by 47°, relative to (a)); (c) electron micrograph of gold decorated lamellae of PBu1 epitaxially oriented on BzAc, with scale bar = 0.2 μm. The BzAc *b*-axis (i.e. the long axis of the needle-shaped substrate crystals) is indicated by a straight arrow. The PBu1 lamellae are thus nearly parallel to the [110] or [$1\bar{1}0$] directions. Note the presence of small domains of thinner lamellae perpendicular to the BzAc *b*-axis (area in lower left part of the picture, indicated by a curved arrow). Inset shows the low-angle diffraction pattern of the large areas with the spots 94° apart; and (d) selected-area diffraction pattern of PBu1, initially epitaxially oriented on benzoic acid as form II, after complete transformation into phase I, due primarily to the result of electron bombardment

Figure 6a illustrates the electron diffraction pattern of PBu1 crystallized on BzAc, while *Figure 6c* shows the lamellar structure of a comparable area as revealed by gold decoration. Two chain and lamellar orientations, 94° apart, are apparent. The diffraction pattern is that of form II of PBuI, as indicated by the small interlayer spacing (and thus large repeat distance i.e. 2.105 nm^{-1}) and the presence of equatorial reflections of spacing 0.77 nm^{-1}, indexed as 200 of form II[5].

The diffraction pattern is complicated by the fact that a significant transformation of form II to form I has already taken place. The presence of form I is manifested by the innermost equatorial reflections (spacing of 0.88 nm^{-1}, indexed as 110) and by additional layer lines, notably the third one (seen as the strongest layer in *Figure 6a*). Exposure to the electron beam enhances the rate of transformation: *Figure 6d* corresponds to the same area after a complete transformation into form I.

The relationship between form II and BzAc can be established by noting that the substrate crystallizes in the form of needles which are elongated in the *b*-axis direction. Combination of morphological (see *Figure 6c*) and diffraction evidence (see *Figure 6a*) therefore leads to the epitaxial relationship depicted in *Figure 6b*, and which can be summarized by:

$$(100)_{\mathrm{PBu,II}} \text{ or } (010)_{\mathrm{PBu,II}} \| (001)_{\mathrm{BzAc}}$$

and

$$c_{\mathrm{PBu,II}} \| [110]_{\mathrm{BzAc}} \text{ or } [\bar{1}10]_{\mathrm{BzAc}}$$

with the $[110]_{\mathrm{BzAc}}$ and $[\bar{1}10]_{\mathrm{BzAc}}$ directions being 94° apart.

A logical lattice match appears to exist between the interchain distance (0.74 nm) and the (110) interplanar distance of BzAc (0.75 nm). The mismatch is -1.3%. A second match exists between the chain axis repeat distance of form II (2.105 nm) and *three* repeat distances along the $\langle 110 \rangle$ diagonal directions of BzAc (0.75 nm),

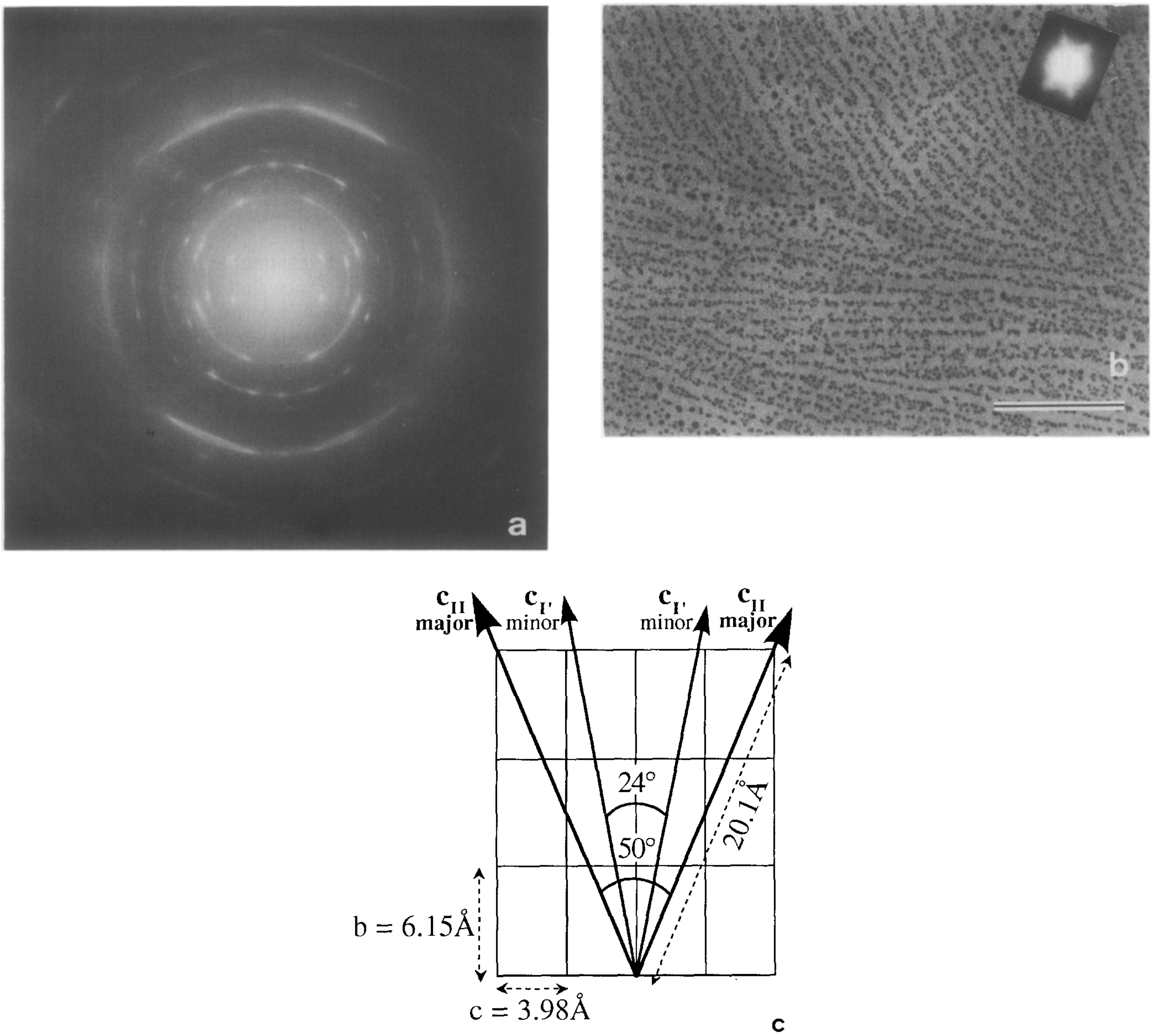

Figure 7 (a) Selected-area diffraction pattern of PBu1 epitaxially grown on 4BrBzAc. Note the two major chain orientations of PBu1, form II, 50° apart, and the minor two chain orientations of PBu1, form I′, 24° apart. The reflections 200 (at 0.745 nm^{-1}) of form II and 300 (at 0.51 nm^{-1}) of form I′ are closest and second closest to the centre of the pattern, respectively; (b) electron micrograph of gold decorated PBu1 lamellae epitaxially oriented on 4BrBzAc, with scale bar = 0.2 μm. Inset shows the low-angle diffraction pattern of such an area, where the lamellar orientations 50° apart can be seen; and (c) schematic representation of PBu1 chain orientations relative to the 4BrBzAc substrate plane

i.e. 2.25 nm (mismatch = −2.1%). This important feature is further analysed when dealing with epitaxy on the 4BrBzAc substrate (see below).

Gold decoration reveals individual domains with single chain and lamellar orientation, which are μm or tens of μm in size (*Figure 6c*). The domains with the two different orientations 94° apart are often interspersed. The domain limits correspond almost always to a single, clearly defined and nearly straight lamellar surface. Lamellar thickness is always significantly larger than for form III: as determined from low-angle selected-area electron diffraction patterns (see inset to *Figure 6c*), the average thickness is ~15 nm.

Finally, it should be noted that a second, different epitaxy of PBu1 on BzAc is revealed by gold decoration: small patches of very thin PBu1 lamellae, parallel to the *a*-axis of BzAc, are observed on certain occasions (indicated by the curved arrow in *Figure 6c*). This phase, however, does not show up in the diffraction patterns. The thickness of these lamellae is comparable to that of form III or form I′.

Figure 7a illustrates the diffraction pattern of PBu1 crystallized epitaxially on 4BrBzAc, while *Figure 7b* shows the lamellar structure as revealed by gold decoration. The epitaxy shares many features in common with that of PBu1 on BzAc. Indeed, it is found that:

(i) mainly form II of PBu1 is obtained;
(ii) the PBu1 contact plane is again (010), as revealed by strong 200 equatorial reflections and;
(iii) part of the sample has already been transformed into form I (cf. again the strongest, third layer lines of form I, and the innermost form I, 110 reflections on the equator).

The main differences are linked with:

(i) a smaller angle between the chain axes orientations of form II, i.e. ~50°, and;
(ii) the existence of a clearly identifiable form I′. This phase shows up mainly as two pairs of reflections (spacing of 0.51 nm) indexed as 300. The two corresponding equators make an angle of 22° and *share with form II a common bisector*.

Analysis of the structural relationship of form II with 4BrBzAc is greatly facilitated by the existence of such double epitaxies (form I′ is considered in a companion paper[8]). The relationship is depicted schematically in *Figure 7c* and can be summarized as follows:

$$(100)_{\mathrm{PBu,II}} \text{ or } (010)_{\mathrm{PBu,II}} \| (100)_{\mathrm{4BrBzAc}}$$

and

$$c_{\mathrm{PBu,II}} \| [032]_{\mathrm{4BrBzAc}} \text{ or } [03\bar{2}]_{\mathrm{4BrBzAc}}$$

with the angle between [032] and $[03\bar{2}]$ calculated as 46.7°.

In the present case, defining the exact lattice match between polymer and substrate becomes a challenge: as suggested by the fairly high Miller indices, no clear-cut substrate periodicities match the polymer interchain distance. However, as for BzAc, a definite dimensional match is again suggested by the similarity of the chain axis periodicity (2.105 nm) and the periodicity of *three* unit cells in the [032] substrate direction, i.e. 2.01 nm (mismatch = +5%). This feature is now analysed in the context of epitaxy of irrational helices.

Epitaxy of irrational helices. Epitaxy of PBu1 as form II on benzoic and 4-bromobenzoic acid provides two related and very illustrative examples of possible interactions of irrational helices. Analysis in molecular terms of polymer–substrate interactions is complicated by the non-crystallographic helix symmetry which precludes repetition of favourable interactions with short periods as are generally assumed in epitaxy.

A few features emerge from these two examples

(i) the role of interchain distance matching is less prominent than for planar zigzag chains. It may still intervene for BzAc (1.5% mismatch with the substrate (110) plane), but not for 4BrBzAc, for which no low index planes match the interchain direction and;
(ii) matching *along the chain axis* repeat is a key feature. This matching involves *three* unit cells of the substrate for both BzAc and 4BrBzAc. It must be related to the 11_3 helix symmetry since the helix (shown in *Figure 8a* in chain axis projection and in *Figure 8b* normal to it) comes into contact three times with the substrate surface per *c*-axis helix repeat distance. In other words, *one helix turn fits one substrate cell periodicity*.

Further analysis of the epitaxy is possible, but is more speculative since it involves more local interactions (which cannot be confirmed experimentally) and also chirality of the helices (which, for form II, cannot be determined from elecron diffraction evidence). The following tentative analysis considers possible interactions of one helical stem.

For a single helix, a reasonable helix axis tilt relative to the subtrate lattice is such that *the helical path becomes nearly parallel to the main substrate features* (in 4BrBzAc, the rows of bromine atoms). This is well established for iPP α-phase epitaxy and homoepitaxy[15,16] and is further amply demonstrated for epitaxy of form I′ in a companion paper[8]. Assuming epitaxy of a helix of the 'proper' hand, one notes that residues 0, 4, and 7 (cf. *Figures 8a* and *8b*) are in contact with the substrate. With adequate helix shifts, they can be made to fit into natural 'niches' of the substrate, for example at the centre of three unit cells (cf. *Figure 8c* where the helix is *under* the substrate). However this analysis does not hold for neighbour helices of opposite hand in the same crystallographic (contact) plane, although crystallographic shifts of helices in the form II unit cell do contribute to favourable local interactions.

To conclude, it is worth re-emphasizing that for irrational helices, the main structural features appear to be the helical path and the interstrand distance, i.e. subunits of the very large chain axis repeat distance. For PBu1 form II, the two observed epitaxies involve parallelism of the helix axes with well defined crystallographic directions to enable matching of a strong substrate structural feature with the helix interstrand distance.

Extension to bulk crystallization

Several exploratory experiments have been performed to check if the direct crystallization of form III can take place in a bulk crystallization process by using 2Qxol as a nucleating agent. Optical microscopy and d.s.c. are not particularly well adapted to these investigations; the overall characteristics of spherulites of different phases are very similar, and the melting and crystallization

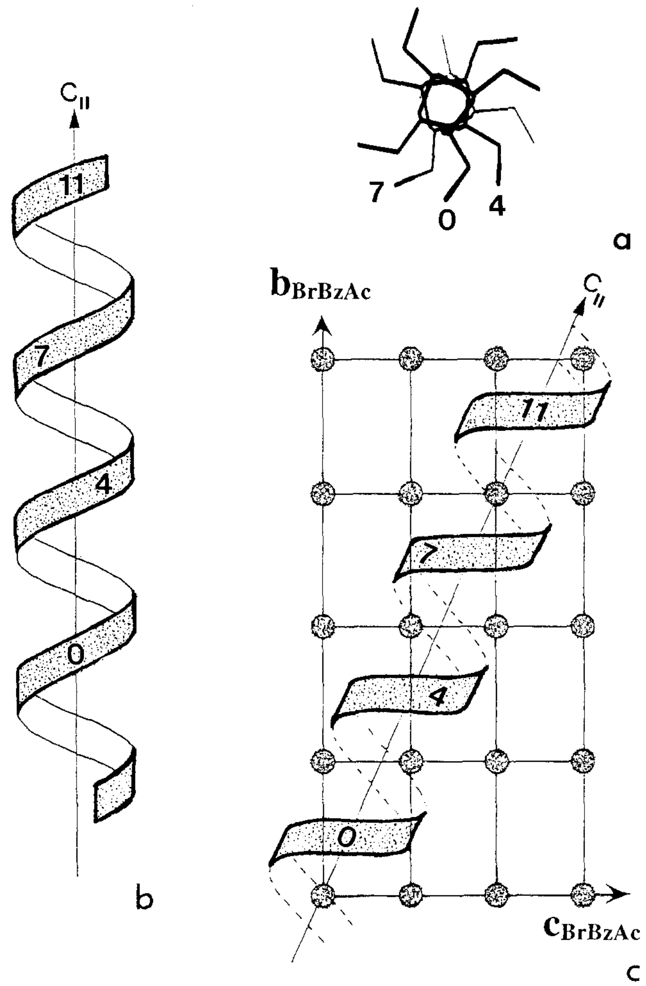

Figure 8 The 11_3 helix conformation of PBu1, form II in: (a) chain axis projection; (b) projection normal to the chain axis and; (c) as deposited on 4BrBzAc. Note that the side chains of residues 0, 4, 7 and 11 interact with the substrate

characteristics are too close to differentiate, e.g. between form III and I′. Wide-angle X-ray diffraction is best adapted for identifying the various phases.

We have observed that a sample of the low-M_w fraction, soaked with a solution of 2Qxol, crystallizes with a significant proportion of form III (linked with the addition of 2Qxol) in addition to the 'natural' form II; form I is produced by transformation of form II. High-M_w polymer does not appear to crystallize as form III, probably due to the higher crystallization temperature range of form II. Indeed, significant development of an unstable phase requires growth rates either equal to, or higher than that of the stable phase at the selected crystallization temperature. This holds true for the β-phase of iPP over the whole 'conventional' crystallization range (105–140°C). By using the appropriate nucleating agents, iPP can therefore be obtained as essentially a pure β-phase, rather than the more conventional α-phase[3].

The search for possible T_c 'windows' in which form III can be produced is the subject of ongoing experiments. However, such windows, if they exist at all, appear to be more limited than for the β-phase of isotactic polypropylene.

CONCLUSIONS

Crystalline polymorphism of PBu1 can be induced in a systematic and consistent manner by epitaxial crystallization on appropriate substrates. Both form III and form I′ (cf. also the companion paper[8]) are obtained, in addition to the naturally occurring form II.

The key feature of 2Qxol (the substrate used to generate form III) is the *matching of its 0.735 nm b-axis periodicity with the 4_1 helix repeat distance of 0.756 nm*. This epitaxy has produced the first oriented pattern of the unstable (to mechanical stress) form III displaying the c^* reciprocal axis (see *Figure 2b*). Investigations with an electron microscope goniometric stage of these epitaxially crystallized films together with studies of single crystals enables exploration of the full reciprocal space of Form III. These data have been used in a reinvestigation of its crystal structure by electron crystallography[17]. Use of 2Qxol as a nucleating agent in bulk crystallization does not produce samples which contain only form III, as a number of additional conditions must be satisfied, for example, proper crystallization range, significant growth rates, etc. Limited success was so far only obtained with a low-M_w fraction.

Epitaxy of form II has been achieved on both benzoic acid and 4-bromobenzoic acid substrates. Analysis of form II epitaxy is complicated by the 11_3 helix symmetry and the long c-axis repeat distance (2.105 nm). The lattice match can be rationalized when considering that the structural unit is the helical turn: *the interturn distance of the irrational helix appears to play the key physical role in the epitaxy*. This statement is further illustrated in a more dramatic form when dealing with epitaxy of form I′, which is reported in a companion paper[8].

ACKNOWLEDGEMENTS

We thank Professors D. Froelich and J. Ladevèze for making their Silicon Graphics station available to us and also for their help, and Dr A. Mathis for performing the X-ray experiments.

REFERENCES

1 Mauritz, K. A., Baer, E. and Hopfinger, A. J. *J. Macromol. Sci. Macromol. Rev.* 1978, **13**, 1
2 Wittmann, J. C. and Lotz, B. *Polymer* 1989, **30**, 27
3 Leugering, H. L. *Makromol. Chem.* 1967, **109**, 204
4 Luciani, L., Seppala, J. and Löfgren, B. *Prog. Polym. Sci.* 1988, **13**, 37
5 Petraccone, V., Pirozzi, B., Frasci, A. and Corradini, P. *Eur. Polym. J.* 1976, **12**, 323
6 Turner-Jones, A. *J. Polym. Sci., Polym. Lett. Edn* 1963, **1**, 455
7 Wittmann, J. C. and Lotz, B. *J. Polym. Sci., Polym. Phys. Edn* 1981, **19**, 1837
8 Kopp, S., Wittmann, J. C. and Lotz, B. *Polymer* 1994, **35**, 916
9 Wittmann, J. C. and Lotz, B. in 'Electron Crystallography of Organic Molecules', (Eds. J. R. Fryer and D. L. Dorset), NATO Series C, Vol. 328, Kluwer Academic, Dordrecht, 1990, p. 241
10 Padmaja, N., Ramakumar, S. and Viswamitra, M. A. *Acta Crystallogr. Sect. C* 1987, **43**, 2239
11 Cojazzi, G., Malta, V., Celotti, G. and Zanetti, R. *Makromol. Chem.* 1976, **177**, 915
12 Bassett, G. A., Blundell, D. J. and Keller, A. *Macromol. Sci. Phys.* 1967, **B1**, 161
13 Bruno, G. and Randaccio, L. *Acta. Crystallogr. Sect. B* 1980, **36**, 1711
14 Okhura, K., Kashino, S. and Haisa, M. *Bull. Chem. Soc. Jpn* 1972, **45**, 2651
15 Lotz, B. and Wittmann, J. C. *J. Polym. Sci., Polym. Phys. Edn* 1986, **24**, 1541
16 Wittmann, J. C. and Lotz, B. *Prog. Polym. Sci.* 1990, **15**, 909
17 Dorset, D. L., McCourt, M., Kopp, S., Wittmann, J. C. and Lotz, B. *Acta Crystallogr.* in press